Electric Power Systems Research 181 (2020) 106186

Contents lists available at ScienceDirect

Electric Power Systems Research

journal homepage: www.elsevier.com/locate/epsr

Statistical inference of multivariable modal stability margins of time-delay perturbed power systems

P. Esquivel[a], G. Romero[b], F. Ornelas-Tellez[c], E.N. Reyes[d], Carlos E. Castañeda[e,*], O.A. Morfin[f,**]

[a] CONACYT-Autonomous University of Tamaulipas, Mexico
[b] Autonomous University of Tamaulipas, Mexico
[c] Universidad Michoacana de San Nicolás de Hidalgo, 58030 Morelia, Mexico
[d] Graduate Studies Program in Electrical Engineering, CINVESTAV-Guadalajara, Jalisco, Mexico
[e] Centro Universitario de los Lagos of the Universidad de Guadalajara, Jalisco, Mexico
[f] Autonomous University of Ciudad Juárez, Chihuahua, Mexico

ARTICLE INFO

Keywords:
Distributed uncertainty
Inter-area stability margins
Multi-scale signal sensitivity
Time-delay perturbed system

ABSTRACT

This paper proposes a modal statistical inference algorithm to define multivariable operational stability limits of time-delay perturbed dynamic systems by employing remote sensor signals. Our proposal overcomes the drawbacks of linear independence and inter-area geometry of time-delays to analyze multiple-input, multiple-output dynamic systems. The manuscript contributes with: (a) the study of stability margins under distributed uncertainty and time-delays for large power systems, (b) the determination of stability conditions of inter-area oscillations through a new probabilistic modeling approach under the influence of intermissions, and (c) the usage of the proposed methodology to derive controlled stability limits and assess the modal resilience of perturbed power systems. Studies on the multi-scale signals sensitivity and multivariable polynomial intersection from empirical perspectives in modal stability analysis are also explored. Results on an IEEE 16-generator 68-bus system are presented to illustrate the effectiveness of the proposed algorithm. The estimation of multivariable operational stability limits and time-delays of inter-area oscillation modes are verified with the vector fitting procedure and first-order Padé approximation.

1. Introduction

Uncertainty and decision analysis are natural conditions at the proper operation of power systems. Today, modern power networks, sometimes with limited operation and control infrastructures, are widespread on large geographical zones. This condition allows proposing new methods of coordination in protection, control, monitoring, and communication to enhance the distributed reliability and security using remote sensor signals. In addition, the time-delay derived by distributed transmission and processing of large datasets have become more relevant in remote operating functions of large networks. Recently, algorithms based on nonlinear Koopman modes [1], adaptive stochastic subspace identification [2], forward and backward extended Prony method [3], dynamic mode decomposition [4], and transient energy metrics [5], have been applied for modeling power systems and monitoring their multivariable modal stability conditions in order to assess the power system health considering measurement data. However, the main enhancements in practical application of these algorithms is to define and ensure operational stability margins of wide-area oscillations when the interconnected systems are subjected to inter-area intermissions and distributed uncertainties. Henceforth, the inter-area intermissions are considered as pre-existing events involving network topology changes, such as scheduled maintenance of generators and power electronic devices, distributed generation and transmission system expansion, the interconnection of isolated systems or international energy cooperation, among others. Several probabilistic analysis methods, as proposed in [6,7], are an effective tool to study power systems with random factors, which mainly aims to derive causal relationship variables intrinsically correlated between them. For instance, [6] has developed a nonlinear analytical method for small-signal stability analysis used to approximate the relationship between modal damping factor ratios and multiple wind generations in a large scope. In [7], a nonlinear contribution method is also derived, which is based on the idea of a sensitivity analysis to identify the fault variables

* Corresponding author.
** Corresponding author.
E-mail addresses: pesquivelpr@conacyt.mx (P. Esquivel), gromero@uat.edu.mx (G. Romero), fornelas@umich.mx (F. Ornelas-Tellez), noereyesp@gmail.com (E.N. Reyes), ccastaneda@lagos.udg.mx (C.E. Castañeda), omorfin@uacj.mx (O.A. Morfin).

https://doi.org/10.1016/j.epsr.2019.106186
Received 11 July 2019; Received in revised form 3 December 2019; Accepted 29 December 2019

after a disturbance is detected. In the method, an independent component analysis is proposed, where dominant process variations are discriminated on the estimated probabilities and assigned with large weights to capture the significant information during online fault detection. Many extensions of statistical methods based on Gaussian mixture models [8], mean spectral radius [9], asymptotic variance [10], k-nearest neighbor analysis [11], and complex empirical orthogonal functions [12], have been developed to improve monitoring performance by taking different process characteristics in consideration. However, these methods only consider the statistical information derived by the system response, without modeling in conjunction the perturbed time-delay and dynamic causality of inter-area intermissions from system stability studies. This condition is considered as a drawback to define coordinated studies of system stability margins in large power systems considering proximity to vulnerability from operating limits. Therefore, an algorithm of prediction and tuning at intelligent decision schemes to centralized monitoring centers should also be developed. Furthermore, the perturbed time-delay derived by distributed transmission and processing of large datasets has become more relevant for predictive stability studies. To address these issues, an adaptive time-delay compensation scheme for a flexible AC transmission system has been suggested in [13]. In this approach, a time-delay compensation technique using Padé approximation has been presented, where it is demonstrated that the performance evaluations are significantly deteriorated without any coordinated time-delay compensation. This fact motivates us to innovate in the present topic. In [14], the delayed communication is compensated by a time-delay compensator designed using Simevents toolbox available with MATLAB, where the geometric measures of controllability and observability, the choice of location and the selection of their respective input signals are obtained. The author in [15] employs a hybrid procedure to design a robust central monitoring system considering distributed uncertainties and resiliency during the permanent failure of remote communication channels. Many researches have contributed to integrate the time-delay in central monitoring schemes defining their operating margins in power system stabilizers (PSS) [16–21]. Their contributions are focused on the feedback signal delay problem derived by route switches or communication load increases, without modeling to detail the distributed uncertainty and inter-area geometry of time-delays to wide-area systems. The incorporation of operational stability limits to time-delay perturbed dynamic systems has been considered as a manner effective to treat the electromechanical oscillations in synchronized power systems. Therefore, a statistical inference algorithm is here proposed to define coordinated modal stability margins employing the dynamic causality of distributed uncertainties and perturbed time-delays in power systems. The method provides a simplified manner to infer modal stability regions for interconnected power systems considering the coordinated operational stability of inter-area intermissions via datasets. Additionally, a probabilistic modeling approach for recognition of empirical redundant-patterns modes is also developed. Therefore, databases of historical information collected during distributed perturbations are here employed to quantify modal resilience in power systems. Thus, regions and margins of dynamic security to inter-area modal instability are inferred as causal relationship forecasting by experticies of past events. Our proposal uses a distributed empirical modeling of time-delay dynamic systems through rational function fitting via datasets, where the uncertainty at both, coefficients of the characteristic equation and perturbed time-delays are analyzed from statistical models. Studies on the multi-scale signals sensitivity and multivariable polynomial intersection from empirical perspectives in modal stability analysis are also explored. Results on an IEEE 16-generator 68-bus system are presented to illustrate the proposed method.

The contributions of this work are:

- The statistical inference of operational stability margins of time-delay perturbed dynamic systems.
- A stability analysis of inter-area oscillations in power systems under a probabilistic approach that considers intermissions.
- The development of an algorithm that quantifies modal resilience by using historical information of faults.

The paper is organized as follows. Section 2 introduces the modeling to time-delay dynamic systems. Section 3 describes the proposed method, where an algorithm to study vulnerability based on the inter-area geometry of perturbed time-delays is presented. Test results and conclusions are given in Sections 4 and 5, respectively.

2. Modeling of time-delay dynamic systems

2.1. General description

Let consider the study of a multivariable time-delay dynamic system, with the following structure [22–25]:

$$\begin{aligned} \dot{\boldsymbol{x}}(t) &= \mathbf{A}_0\boldsymbol{x}(t) + \sum_{j=1}^{\eta} \mathbf{A}_j\boldsymbol{x}(t-\tau_j) + \mathbf{B}\boldsymbol{u}(t) \\ \boldsymbol{y}(t) &= \mathbf{C}\boldsymbol{x}(t) \end{aligned} \tag{1}$$

where $\mathbf{A}_0$, $\mathbf{A}_j$ are matrices, $\mathbf{B}$ and $\mathbf{C}$ are vectors of appropriate dimensions, and τ_j with $0 < \tau_1 < \tau_2 < \cdots < \tau_\eta$ is a real positive number used to quantify time-delays, whereas $\boldsymbol{x}(t) \in \mathbb{R}^m$, $\boldsymbol{y}(t) \in \mathbb{R}^n$, $\boldsymbol{u}(t) \in \mathbb{R}^q$ are the state vector, the output and the input of the system, respectively. The stability of the system (1) is determined by the loci of the roots of the characteristic equation:

$$\det(s\boldsymbol{I} - \mathbf{A}_0 - \sum_{j=1}^{\eta} \mathbf{A}_j e^{-\tau_j s}) = 0, \quad \forall\, s \in \mathbb{C}_+, \quad (\eta \le m) \tag{2}$$

with $\mathbb{C}_+$ delimiting the set of complex numbers, *i. e.*, $s = -\sigma + i\omega$, of lesser or real part equal to zero, while the operator $\forall$ indicates the universal quantifier. Although new methods have been proposed to infer the guaranteed stability regions of (1), such as those outlined in [22–25], the modal stability problem under distributed uncertainty and perturbed time-delay in multimachine power systems is still an open research topic. Essentially, the stable system condition using time-synchronized measurements and historical databases have been poorly explored employing these methods. With the rapid advancements in synchronized phasor measurement technologies, developing novel multivariable stability monitoring algorithms for inter-area electromechanical oscillations has become a hot topic in recent years. Several works reported in [1–5], which involve a recursive analysis of eigenvalue movements from Hurwitz matrices, have been carried out to measure the modal dynamic stability. However, one of the main enhancements in the practical application of these algorithms is to define and ensure margins, by causal relationships prediction, of the multivariable modal stability under distributed uncertainties and perturbed time-delays. Thus, in this paper is proposed new studies to define inter-area modal stability margins and monitoring using empirical approaches as models. From time-synchronized measurements obtained by system response, the multi-scale signals sensitivity, perturbed time-delays, and distributed dynamic causality are treated in conjunction to derive guaranteed regions of dynamic security under multivariable modal instability conditions for interconnected power systems.

2.2. Problem formulation

Let us define the dynamic response of system (1) as:

$$\boldsymbol{y}(t) = \boldsymbol{y_h}(t) + \boldsymbol{y_p}(t) \tag{3}$$

with $\boldsymbol{y_h}(t)$ and $\boldsymbol{y_p}(t)$ denoting the response of the homogeneous and non-homogeneous part, respectively, of the linear system. It is well-known that the dynamic response associated to j-th system input of (1),

i.e., $\boldsymbol{y}_j(t)$ can be fitted in a linear combination of L parametric signals at rational functions from the frequency domain, with the form of (3), as follows [22]:

$$\begin{aligned}\boldsymbol{y}_j(s) &= \boldsymbol{y}_h(s) \cup \boldsymbol{y}_p(s) \\ &= \sum_{k=1}^{L} \{\frac{\mathbf{r}_k}{s-a_k} \cup \frac{\Delta\mathbf{r}_k}{(s-a_k)(1-e^{-\tau_j s})}\} + \boldsymbol{\varepsilon}_j(s), \quad (L \le m)\end{aligned} \tag{4}$$

where $\cup$ denotes the union set relation, and $\boldsymbol{\varepsilon}_j(s) = (\boldsymbol{d} \cup \Delta\boldsymbol{d}) + s(\boldsymbol{h} \cup \Delta\boldsymbol{h})$. For (4), the poles $\{a_k\}$ and the residues $\{\mathbf{r}_k\}$ are either real or complex conjugate pairs, $\boldsymbol{d}$, $\boldsymbol{h}$ are real coefficient matrices, whereas the operator Δ accordingly denotes the changes at nominal operating points or the uncertainty of (1). Therefore, the aim of this paper is to determine the conditions under which the dynamical responses of (1) becomes stable considering multiple system inputs by using a proper rational equivalent model with the form of (4). To this end, it is essential to consider that

$$\boldsymbol{y}_h(s) = \frac{D_h(s)}{M(s)} = \sum_{k=1}^{L} \frac{\mathbf{r}_k}{s-a_k} \tag{5}$$

and

$$\boldsymbol{y}_p(s) = \frac{D_p(s)}{M(s)(1-e^{-\tau_j s})} \tag{6}$$

are proper rational function approximations of (1) with form (4) fitted from its dynamic response in the frequency domain, where $D_p(s) = D_h(s) - D_h(s)e^{-\tau_j s}$, with $D(s)$, $M(s)$ denoting the numerator and denominator polynomial, respectively. In this approach, we assume that (5) and (6) are strictly proper rational functions in the sense of linear system theory, which is considering no response at $\boldsymbol{y}(t) \to \infty$ with asymptotic value $\boldsymbol{d} = 0$, *i. e.*, $\varepsilon(s) = 0$.

In order to delimit the piecewise linear models from (6), the poles at $1/(1-e^{-\tau_j s})$ can be estimated considering that $e^{-\tau_j s} = \cos(\tau_j\omega) - i\sin(\tau_j\omega) = 1$ at $\tau_j\omega = \pm 2n\pi$ for $(n = 0, a, b, ...)$, and $\sigma = 0$; thereby, the poles are mapping on the complex plane in $s = \pm i2n\pi/\tau_j$. Thus, the proximity and movements to points (holes) of instability at time-delay dynamic systems can be defined by the loci of the roots from the denominator polynomial function $p(s, \tau_j) = M(s)(1-e^{-\tau_j s}) \neq 0$, in the interval $s = \{(-i2\pi/\tau_j, 0) \cup (0, i2\pi/\tau_j)\}$, where

$$\lim_{s \to \pm i(2n\pi)/\tau_j} s\boldsymbol{y}_p(s) \to 1/\left(1-e^{-\tau_j s}\right) \tag{7}$$

as it is illustratively shown in Fig. 1. It is sufficient to define that in $\tau_j = 0$, $\boldsymbol{y}_p(s) = \{\varnothing\}$, with symbol $\{\varnothing\}$ denoting the empty set. Then, it should be noticed that the parametric variations at controlled conditions of (1), *i. e.*, the amplitude of the coefficients of the characteristic equation and time-delays between some interval, regions and margins of dynamic security during inter-area modal instability by causal relationships might be forecasted, so that variables intrinsically correlated between them can be derived.

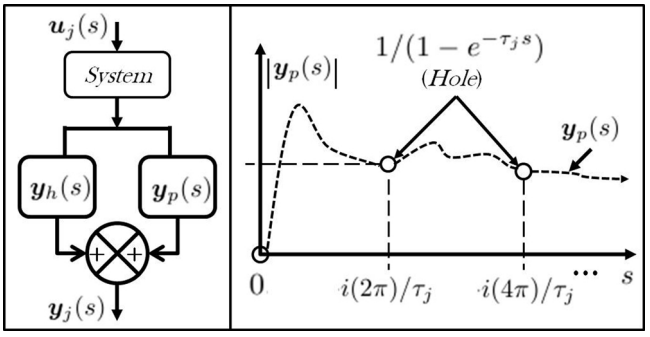

Fig. 1. Left: Equivalent diagram. Right: Piecewise dynamic responses.

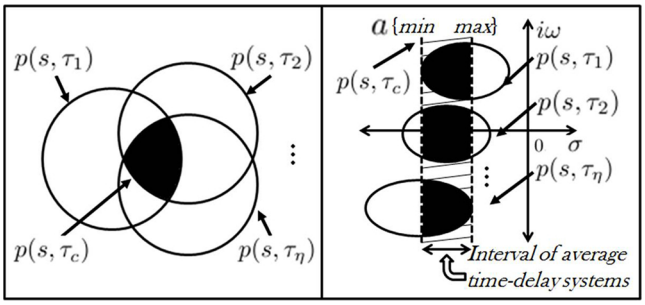

Fig. 2. Polynomial intersection set relation. Left: Region generated. Right: Loci of the roots.

3. Proposed method

3.1. Multivariable polynomial intersection

In what follows, it is important noting that in case of multiple system outputs with random spatial distribution of their input signals, the k-th rational function fitting of $\boldsymbol{y}_p(s, \tau_1 ...\tau_\eta)$, in the interval $s = \{(-i2\pi/\tau_j, 0) \cup (0, i2\pi/\tau_j)\}$, is modeled from (4) as:

$$\boldsymbol{y}_p(s, \tau_1 ...\tau_\eta) = \left\{\frac{\bigcup_{j=1}^{\eta} \Delta_j \mathbf{r}_k}{\bigcup_{j=1}^{\eta}(s-a_k)(1-e^{-\tau_j s})}\right\}. \tag{8}$$

Therefore, to infer the stability region and conditions generated by variation of the coefficients a_k and τ_j in some intervals during distributed perturbations of causal relationships, it is sufficient to check the family of multivariable polynomials with spectral overlap [22–25]. Roughly speaking, it is considered that $p(s, \tau_c)|_{s \to a_k} = \{p(s, \tau_1) \cap p(s, \tau_2) \cap ... \cap p(s, \tau_\eta)\} \neq 0$, with $\cap$ denoting the polynomial intersection set relation, is associated to a stable region of time-delay perturbed systems which is depending of the linear combinations with common factor τ_c in $\{\tau_1 \cup \tau_2 \cup ... \cup \tau_\eta\}$. This is illustratively shown in Fig. 2.

Essentially, $p(s, \tau_j) = M(s, a)(1-e^{-\tau_j s})$, with $M(s, a) = \kappa_n s^n + \kappa_{n-1}s^{n-1} + ...\kappa_1 s + \kappa_0$ of arbitrary polynomial order n, constant coefficients κ and roots $\{a_k\}$, briefly introduces the development of the problem described above. It is worth pointing out that the method of the frequency-domain empirical orthogonal functions (FD-EOFs) has been used in this paper to design the polynomial intersection set relation and its linear independence [26–28]. Thereby, having time-domain data series, these are transformed to frequency-domain data series using algorithms based in the Fourier transform [29]. Therefore, considering multiple system inputs, their multiple responses are included as a two-dimensional array with data structure $\boldsymbol{Y}_p(x_j, \omega)$, as follows:

$$\boldsymbol{Y}_p(x_j, \omega) = [\boldsymbol{y}_p^{\top}(s, \tau_1), \boldsymbol{y}_p^{\top}(s, \tau_2), ...\boldsymbol{y}_p^{\top}(s, \tau_\eta)] \tag{9}$$

where x_j to $j = 1, 2, ...,\eta$ represents the spatial distribution of sensors in variable data fields; whereas the superscript $\top$ denotes vectorial transposition. Thus, the optimal decomposition of (9) using FD-EOFs is approximated in a linear combination of Q proper orthogonal modes from both optimal orthogonal eigenfunctions $\boldsymbol{\varphi}(x)$, and spectral coefficients $\mathbf{v}(\omega)$ of average-inertia frequency, for the q-th partial model according to [26–28], as:

$$\boldsymbol{Y}_p(x, \omega) \triangleq \sum_{q=1}^{Q} \mathbf{v}_q(\omega)\boldsymbol{\varphi}_q^H(x), \quad (Q \le m) \tag{10}$$

for all $\omega \in \mathbb{R}$, and with the superscript H denoting complex conjugation of a complex matrix. In the method, the optimal spatial basis functions $\boldsymbol{\varphi}_q(x)$ are obtained as the orthogonal eigenvectors of a cross-spectral matrix $\mathbf{C}_\omega(x) \in \mathbb{C}$, *i. e.*

$$\mathbf{C}_\omega(x) = \boldsymbol{Y}_p(x, \omega)\boldsymbol{Y}_p^H(x, \omega) \tag{11}$$

by solving the eigenvalue problem with form

$$\mathbf{C}_{\omega}(x)\boldsymbol{\varphi}_q(x) = \lambda\boldsymbol{\varphi}_q(x) \tag{12}$$

where $\boldsymbol{\varphi}_q(x)$ is the eigenfunction corresponding to the eigenvalue λ_q of a particular bandwidth with spectral energy overlap in $0 < \lambda_1 < \lambda_2 < \ldots < \lambda_Q$. Furthermore, by orthonormality condition and using the property of the inner product, one obtains that

$$\mathbf{v}_q(\omega) = \langle \boldsymbol{\varphi}_q(x), \mathbf{Y}_p(x, \omega)\rangle. \tag{13}$$

Additionally, it can be shown that the eigenvalues of $\mathbf{v}_q(\omega)$, *i.e.* $\lambda_q = \langle \|\mathbf{v}_q(\omega)\|^2\rangle$, where $\|\cdot\|$ is the L^2-norm, and $\langle\cdot\rangle$ implies the use of an average operation, is also a measure of how much the mode participates in generating the system response. Then, the coefficients $\mathbf{v}_q(\omega)$ of average-inertia frequency can be fitted in a proper rational function model with form [22,28,30]:

$$\mathbf{v}_q(\omega) = \sum_{k=1}^{L} \frac{\tilde{r}_k}{s - \tilde{a}_k} = \frac{d_q(s)}{p_q(s, \tau_c)} \tag{14}$$

where the denominator polynomial $p_q(s, \tau_c) = \prod_{k=1}^{L}(s - \tilde{a}_k)$, with tilde ($\sim$) symbol denoting estimated value, is a common factor of multivariable polynomials at $\{p(s, \tau_1) \cap p(s, \tau_2) \cap \ldots \cap p(s, \tau_\eta)\}$, e.g., $p_q(s, \tau_c)|_{s\to\{\tilde{a}_k\}} \neq 0$, with sensitivity:

$$\frac{1 - \lambda_q}{\lambda_q} + \frac{p_q(s, \tau_c)}{p(s, \tau_j)} \neq 0. \tag{15}$$

Hence, it is derived that

$$\tilde{\mathbf{Y}}_p(x, \omega) = \sum_{q=1}^{Q}\sum_{k=1}^{L} \frac{\tilde{\mathbf{r}}_k}{s - \tilde{a}_k} = \sum_{q=1}^{Q} \frac{\tilde{D}_{p(q)}(s)}{p_q(s, \tau_c)}, \quad (Q, L \leq m) \tag{16}$$

with $\tilde{\mathbf{r}}_k = \tilde{r}_k\lambda_q\boldsymbol{\varphi}_q^H(x)$. Consequently, it is possible to obtain an equivalent linear state-space model through (16) using a diagonal canonical representation, where studies regarding to sensor optimal locations and system observability analysis can be developed as described in [10,14,15,31,32]. Thus, in order to define the dissipativity analysis and inter-area geometry of perturbed time-delays under modal stability conditions using this approach, we consider that $p_q(s, \tau_c)$ has the form $p_q(s, \tau_c) = M_q(s, \tilde{a})(1 - e^{-\tau_{c(q)}s})$, $\forall\ \tau_{c(q)} \in \{\tau_1 \cup \tau_2 \cup \ldots \cup \tau_\eta\}$ of stable interval $\tau_{c(q)} = [\tau_{\min}, \tau_{\max}]$, as it was illustrated in Fig. 2. This approach overcomes the drawbacks of computational burden, optimization criterion, orthogonality condition, linear independence, and inter-area geometry of time-delays to analyze through conventional methods the characteristic equation of multiple-output, multiple-input dynamic systems, for instance, presented in [22–25,33].

3.2. Multi-scale signal sensitivity analysis

It can be seen from (12) that $\lambda \in (0, 1]$, with conditions:

$$\lambda_q > 0, \quad \sum_{q=1}^{Q} \lambda_q = 1 \tag{17}$$

and that this has a spectral energy distribution (SED) given by

$$\mathrm{SED}(\lambda_q) = \frac{\lambda_q}{\sum_{q=1}^{Q}\lambda_q}. \tag{18}$$

Additionally, it is noticed that $p_q(s, \tau_c)$ in (16) is an orthogonal subspace in $\{p(s, \tau_1) \cap p(s, \tau_2) \cap \ldots \cap p(s, \tau_\eta)\}$ denoted by operator $\mathcal{R}^{\perp}$, *e.g.*, $\mathcal{R}\{p_q(s, \tau_c)\}^{\perp} \subseteq \mathcal{R}\{p(s, \tau_1) \cap p(s, \tau_2) \cap \ldots \cap p(s, \tau_\eta)\}$, of property $a_c = -\sigma_c + \omega_c e^{i\pi/2}$, with $a_c = \{\tilde{a}_k\}$ and $\sigma_c > 0$, where the superscript $\perp$ denotes the orthogonal condition. Hence, by assuming that $p_q(s, \tau_c)$ and $p(s, \tau_j)$ are stables, essentially with spectral symmetries overlapped in $\lambda_q \approx e^{-\tau_{c(q)}s}$ derived from (12), it is shown the multi-scale signal sensitivity and inter-area geometry of perturbed time-delays to dynamic systems for:

$$\Delta p(s, \tau_j) = (1 - \lambda_q)p(s, \tau_j) + \lambda_q p_q(s, \tau_c) \neq 0 \tag{19}$$

where $\Delta p(s, \tau_j)$ denotes a set of independent polynomial coefficients among perturbations under uncertainties spatially distributed. Therefore, the first order (eigenvalue) spectral energy sensitivity is given by $\Delta\lambda/\Delta p(s, \tau_j)$. Thus, the stability regions can be established by considering phase shifting and movements of $p(s, \tau_j)$ regarding to $p_q(s, \tau_c)$; being it a main contribution presented in this paper. The analysis above indicates that the proposed approach describes a more general class of linear perturbations or it can be used to approximate nonlinear (including multilinear) perturbations among interconnected subsystems.

3.3. Modal stability approach of time-delay perturbed dynamic systems

Given a finite number of open-loop transfer functions $\boldsymbol{G}_j(s, \tau) = \boldsymbol{y}_h(s) \cup \boldsymbol{y}_p(s)$ for $j = 1, 2, \ldots, \eta$, and an uncertainty model consisting of all linear combinations:

$$\boldsymbol{G}(s, \tau) = \sum_{j=1}^{\eta} \lambda_j \boldsymbol{G}_j(s, \tau), \qquad \sum_{j=1}^{\eta} \lambda_j = 1 \tag{20}$$

the stability of the closed-loop system with a unit feedback can be reduced to the multivariable analysis from the denominator polynomials expressed as:

$$\boldsymbol{P}(s, \tau) = \{(\boldsymbol{G}_1(s, \tau) + 1)p_1(s, \tau) \cap \ldots \cap (\boldsymbol{G}_\eta(s, \tau) + 1)p_j(s, \tau)\} \tag{21}$$

where $p_j(s, \tau)$ is the least common denominator of $(\boldsymbol{G}_j(s, \tau) + 1)$ [22,32]. Suppose now that the coefficients of $p_j(s, \tau)$ in (21) involve uncertain parameters with form (19), then it is of interest to determine the stability regions of the system for all admissible perturbations. Thus, from the proposal described into subsections 3.1 and 3.2, it is assumed that there exists a common factor $p_j(s, \tau_c) \in \{p_1(s, \tau) \cap p_2(s, \tau) \cap \ldots \cap p_\eta(s, \tau)\}$ of stable conditions to each λ_j in (20) by decomposition in FD-EOFs, such that $\boldsymbol{P}(s, \tau)$ might be written as:

$$\boldsymbol{P}(s, \tau) = \{\boldsymbol{P}(s, \tau_c)\} \cup \{\Delta\boldsymbol{P}(s, \tau)\}^{\perp} \tag{22}$$

where with form (4), it is straightforward to show that:

$$\boldsymbol{G}(s, \tau) = \{\boldsymbol{G}(s, \tau_c)\} \cup \{\Delta\boldsymbol{G}(s, \tau)\}^{\perp}. \tag{23}$$

Note that in this approach, the polynomial intersection is considered, for which $\boldsymbol{P}(s, \tau_c)$ is derived, as the linear combinations of a family of multivariable polynomials spatially distributed and of stable conditions to generalize the inter-systems stability. Therefore, the stability problem of $\boldsymbol{G}(s, \tau)$ in (23) becomes a special case of multivariable linear systems, where the loci of all roots to each polynomial in $\boldsymbol{P}(s, \tau)$ must be guaranteed in the open left-half complex plane and adjusted to be passive ensuring numerical stability, *e. g.*, $\mathrm{eig}(\mathrm{Re}\{\boldsymbol{G}(s, \tau)|_{s\to a_k}\}) > \{0\}$ to $a_k = -\sigma_k + i\omega_k$ with $\sigma_k > 0$ [34,35]. Thus, the stability of this model is ensured by defining that the dynamic response based at perturbations lead to stable regions, is to say, to post-disturbance steady-state operating points under base frequency conditions (natural modes) and operating equilibrium. For understanding how multiple inputs excite the natural dynamics of the systems, maybe altering its stability condition, in this paper is explored the relation of multivariable function composition described by:

$$\{(\boldsymbol{f}\circ\boldsymbol{g})(s)\} = \{\boldsymbol{f}(s)|_{s=\boldsymbol{g}(s)}\} = \{\hbar(s)\} \tag{24}$$

where the operator ($\circ$) denotes the composition relation $\hbar(s)$ between arbitrary functions $\boldsymbol{f}(s)$ and $\boldsymbol{g}(s)$ [36]. With the definition above, it should be noticed that if and only if $\mathcal{R}\{\boldsymbol{g}(s)|_{s=a_c}\}^{\perp} \subseteq \mathcal{R}\{\boldsymbol{f}(s)|_{s=a_c}\}$, then $a_c \in \{\boldsymbol{f}(s) \cap \boldsymbol{g}(s)\}$. Thus, the proximity and movements to system instability points from the distributed uncertainty are treated by considering a detailed analysis to (22) with form (24), as follows:

$$\{\boldsymbol{P}(s, \tau)|_{s\to\{\tilde{a}_k\circ\Delta a_k\}}\} = \{\{\boldsymbol{P}(s, \tau_c)|_{s\to\{\tilde{a}_k\}}\}\circ\{\Delta\boldsymbol{P}(s, \tau)|_{s\to\{\Delta a_k\}}\}^{\perp}\} \neq \{0\}. \tag{25}$$

Given that $\{\boldsymbol{P}(s,\tau)|_{s\to\{a_k\}}\}\neq\{0\}$ in pre-disturbance steady-state operating points, then it is assumed that the loci of all roots of $\{\boldsymbol{P}(s,\tau_c)\}$ are guaranteed in the open left-half complex plane, *e. g.*, $\{\prod_{k=1}^{L}(s-\tilde{a}_k)|_{s\to\{\tilde{a}_k\}}\}\neq\{0\}$ with $-\tilde{\sigma}_k<0$. To the case in that $\{\Delta\boldsymbol{P}(s,\tau)|_{s\to\Delta a_k}\}\neq\{\varnothing\}$, the condition (25) can be defined under the following restriction:

$$\mathcal{R}\{\Delta\boldsymbol{P}(s,\tau)|_{s\to\Delta a_k}\}^{\perp}\subseteq\mathcal{R}\{\{\boldsymbol{P}(s,\tau_c)|_{s\to\tilde{a}_k}\}\neq\{0\}\}. \tag{26}$$

Thus, to obtain the stability condition of (23) using the real and imaginary part of $\{\boldsymbol{P}(s,\tau_c)|_{s\to\tilde{a}_k}\}$ and $\{\Delta\boldsymbol{P}(s,\tau)|_{s\to\Delta a_k}\}^{\perp}$, hereafter denoted by Re and Im respectively, it is convenient to write that:

$$\begin{aligned}\{\boldsymbol{P}(s,\tau_c)|_{s\to\tilde{a}_k}\} &= m_c+n_c\\ \{\Delta\boldsymbol{P}(s,\tau)|_{s\to\Delta a_k}\}^{\perp} &= m_\Delta+n_\Delta\end{aligned} \tag{27}$$

where $\{m_c, m_\Delta\}$ and $\{n_c, n_\Delta\}$ are the even and odd parts of the polynomial functions in s. Then, we have that the multivariable function composition is given by:

$$\{\boldsymbol{P}(s,\tau)|_{s\to\{\tilde{a}_k\circ\Delta a_k\}}\}=\{\{m_c+n_c\}\circ\{m_\Delta+n_\Delta\}\}, \tag{28}$$

with

$$\mathrm{Re}\{\boldsymbol{P}(s,\tau)|_{s\to\{\tilde{a}_k\circ\Delta a_k\}}\}=\{\{m_c\circ n_\Delta\}+\{n_c\circ m_\Delta\}+\{n_c\circ n_\Delta\}\} \tag{29}$$

and

$$\mathrm{Im}\{\boldsymbol{P}(s,\tau)|_{s\to\{\tilde{a}_k\circ\Delta a_k\}}\}=\{m_c\circ m_\Delta\}. \tag{30}$$

Therefore, as it was illustrated in Fig. 1 and defining that $\theta(s,\tau)=\tan^{-1}(\mathrm{Im}\{\boldsymbol{P}(s,\tau)\}/\mathrm{Re}\{\boldsymbol{P}(s,\tau)\})$ represents the phase angular of $\{\boldsymbol{P}(s,\tau)\}$, by checking whether

$$\begin{aligned}e^{-\tau_c s}|_{s\to\{\tilde{a}_k\circ\Delta a_k\}} &= \cos\left(\left\{\theta(s,\tau)|_{s\to\{\tilde{a}_k\circ\Delta a_k\}}\right\}\right)-i\cdot\sin\left(\left\{\theta(s,\tau)|_{s\to\{\tilde{a}_k\circ\Delta a_k\}}\right\}\right)\\ &= 1,\end{aligned}$$

in the interval $s=\{(-i2\pi/\tau_c,0)\cup(0,i2\pi/\tau_c)\}$, the modal stability property of (23) can be assessed. In addition, graphical tests of operational stability regions by the loci of the roots of the polynomial function $\{\boldsymbol{P}(s,\tau)|_{s\to\{\tilde{a}_k\circ\Delta a_k\}}\}$ can also be generated. The derivation of (29) and (30) are associated with the distributed dynamic causality of inter-area intermissions from the proposed approach. Note that the intervals to varying the coefficients $\tilde{a}_k(s)$ and time-delays τ_c at a guaranteed region of controlled stability conditions are given by $\{(\tilde{a}_k(s)-\Delta a_k(s))\le\tilde{a}_k(s)\le(\tilde{a}_k(s)+\Delta a_k(s))\}$ and $\{\tau_{\min}\le\tau_c\le\tau_{\max}\}$, respectively.

3.4. Statistical representation of the operational stability condition

In order to give a deeper insight of stability conditions in time-delay perturbed power systems using statistical representations, it is assumed that a spectral model overlap with mixture components occurs, as proposed in [6,8,12]. Thus, a parametric-probability density function represented as a weighted sum of multiple averaged densities, to a set of hidden random variables x, is presented as:

$$\boldsymbol{f}_d(x)=\sum_{j=1}^{\eta}\left\{\rho_j\sqrt{\frac{1}{2\pi\beta_x^2}}\exp\left[-\frac{1}{2}\left(\frac{x-\mu_c}{\beta_x}\right)^2\right]\right\} \tag{31}$$

to $\sum_{j=1}^{\eta}\rho_j=1$, where each component has three sets of parameters: weight (ρ_j), average mean (μ_c), and standard deviation (β_x). Thus, the parameters to characterize (31) are selected from (20) as $\rho_j\equiv\lambda_j$, $\mu_c=\|\{\boldsymbol{P}(s,\tau_c)|_{s=\tilde{a}_k}\}\|$, $\beta_x=\|\{\boldsymbol{P}(s,\tau_c)|_{s=\tilde{a}_k\circ\Delta a_k}\}\|$, respectively. Thereafter the joint-probability distribution function with respect to random changes at a selected equilibrium point is consequently constructed. The method operates by selecting the component with the largest weight as the principal component to generate a cluster of data under modal stability conditions and merging all components that fall on a particular bandwidth having spectral energy overlap. Therefore, the probabilistic modeling of the distributed modal stability here developed also represents a novel contribution in this paper. The adopted approach in (31) is a widely-used technique for modeling probabilistic uncertainties with multivariate distribution in power systems. A more detailed discussion on the development of this method can be found in references [6,8].

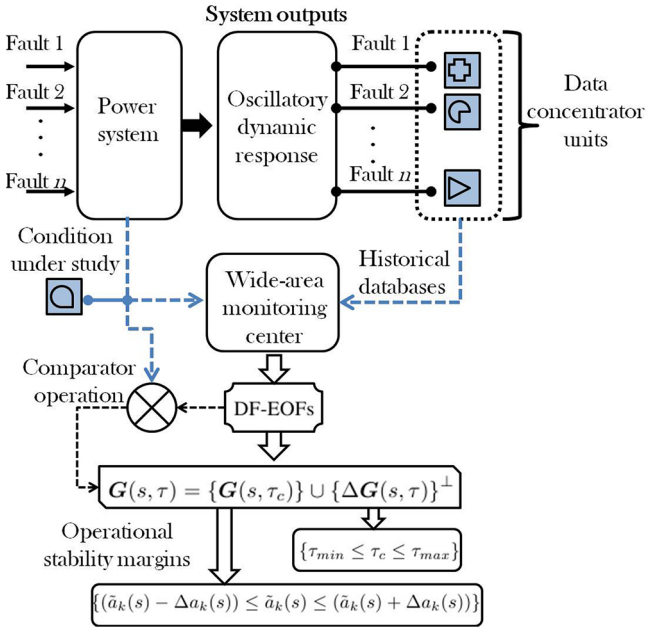

Fig. 3. Proposed algorithm to the stability analysis of perturbed systems.

3.5. Proposed algorithm

The proposed method is illustrated in Fig. 3, which is summarized step-by-step as follows:

1. Consider the databases of historical information collected during distributed perturbations in power systems.
2. Determine a rational equivalent model by empirical response fitting of average-inertia frequency.
3. Estimate the independent polynomial coefficients among perturbations under distributed uncertainties.
4. Define the intervals to varying the coefficients $\tilde{a}_k(s)$ and time-delays τ_c at a guaranteed region of controlled stability conditions.
5. Assessing the system stability region at an arbitrary operating point.

Thus, the following considerations are introduced from it:

- It is assumed that there is spatial overlap among measurement data.
- The time step remains fixed during the process of data collection by sensors.
- The arrays are databases of the same variable and spatio-temporal dimension.
- The power system under study will not have unknown changes in its structure to consider historical perturbations.

4. Performance evaluation

4.1. Illustrative case

This section provides an illustrative test to define the properties of the proposed method. The linear system here employed is described in [24] as:

$$\begin{aligned}\dot{\boldsymbol{x}}(t) &= \mathbf{A}_0\boldsymbol{x}(t)+\mathbf{A}_\Delta\boldsymbol{x}(t-\tau)+\mathbf{B}\boldsymbol{u}(t)\\ \boldsymbol{y}(t) &= \mathbf{C}\boldsymbol{x}(t)\end{aligned} \tag{32}$$

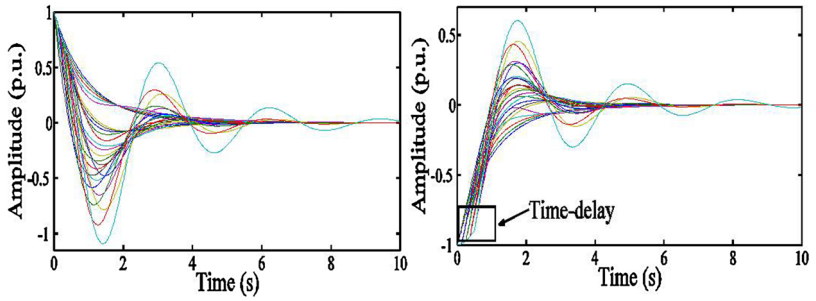

Fig. 4. Time-domain system response associated with multiple parametric uncertainties. Left: state 1. Right: state 2.

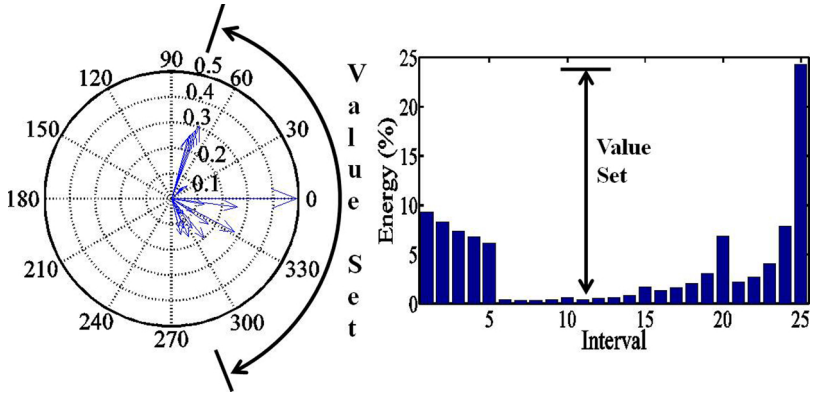

Fig. 5. Variations associated to modal stability conditions in the interval {[0, 2] ∪ (0, 0.5]}. Left: mode shape. Right: spectral energy.

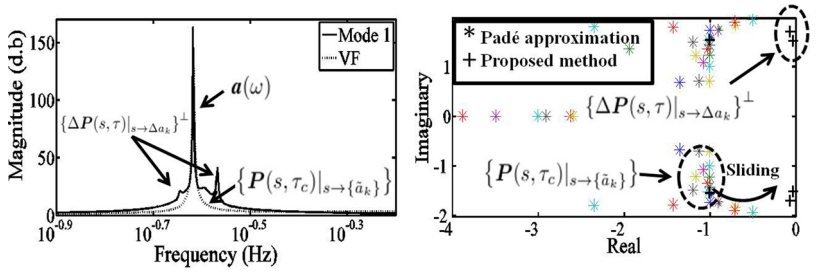

Fig. 6. Movements to the loci of the roots in the complex plane. Left: spectral coefficient. Right: Loci of the roots.

where

$$\mathbf{A}_0 = \begin{bmatrix} 0 & 1 \\ -1 & -1 \end{bmatrix}, \quad \mathbf{A}_\Delta = \begin{bmatrix} 0 & q \\ 0 & -1 \end{bmatrix},$$
$$\mathbf{B} = [1, 1]^\top, \quad \mathbf{C} = [1, 1].$$

Therefore, system (32) has uncertainty in the parameter $q \in [0, 2]$ and also in the delay $\tau \in (0, 0.5]$, of the characteristic equation:

$$\det(s\boldsymbol{I} - \boldsymbol{A}_0 - \mathbf{A}_\Delta e^{-\tau s}) = 0 \quad \forall\, s \in \mathbb{C}_+. \tag{33}$$

Developing this equation, the following multivariable polynomial function is obtained:

$$p(s, \tau) = s^2 + s + 1 + (s + q)e^{-\tau s}, \quad q \in [0, 2], \tau \in (0, 0.5]. \tag{34}$$

For testing the procedure described in Section 3, 25 equally spaced points in the interval $\{q \cup \tau\} = \{[0, 2] \cup (0, 0.5]\}$ are applied to (32), and 1024 time samples into the range $t = [0, 10]$ seconds are used. By illustration, the impulse function is defined as its input signal. In Fig. 4 are shown their dynamic responses associated to multiple system outputs, where the variations caused by the parametric uncertainty are mapping as time-domain data series. Then, an array consisting of a collection of dynamic measurements with form (9) and of dimension 50×1024 is structured. Thus, the proposed method is validated employing frequency-domain data series, which are derived from time-domain measurements. This step is developed using algorithms based on the Fourier transform. It should be noticed that the cross-spectral between multivariable functions are correlations of spatial variations at phase shifting and amplitude derived through optimal basis functions, *e. g.*, these are scattered as movements in its spectral mode shape estimated from the orthogonal eigenvector, $\boldsymbol{\varphi}(x)$, accordingly to (10). Therefore, in Fig. 5 are shown the phase shifting distribution and amplitude estimated to the dominant-inertia frequency mode, where the contributions of spectral energy are also illustrated. From Fig. 5, note that the eigenvectors showing the mode shape variations are generators of every $\boldsymbol{G}_j(s, \tau)$ under parametric uncertainty. Thus, when the magnitude of every vector $\boldsymbol{\varphi}(x)$ does not vanish, this is equivalent to the assumption that the set of the multivariable coefficients of the generators $\boldsymbol{G}_j(s, \tau)$ are on one side of some line through the origin in the plane complex. For the case of modal stability analysis using $\boldsymbol{P}_j(s, \tau)$, this requires that the multivariable coefficients of $\boldsymbol{G}_j(s, \tau)$ have the same direction between them with spectral overlap at a particular bandwidth. Hence, to verify whether all roots of every polynomial function in (34) belong to a guaranteed region of dynamic security, it is validated from results derived by application of a vector fitting (VF) procedure [28], and results previously presented in reference [24] by first-order Padé approximation. Regarding to stability conditions, results are

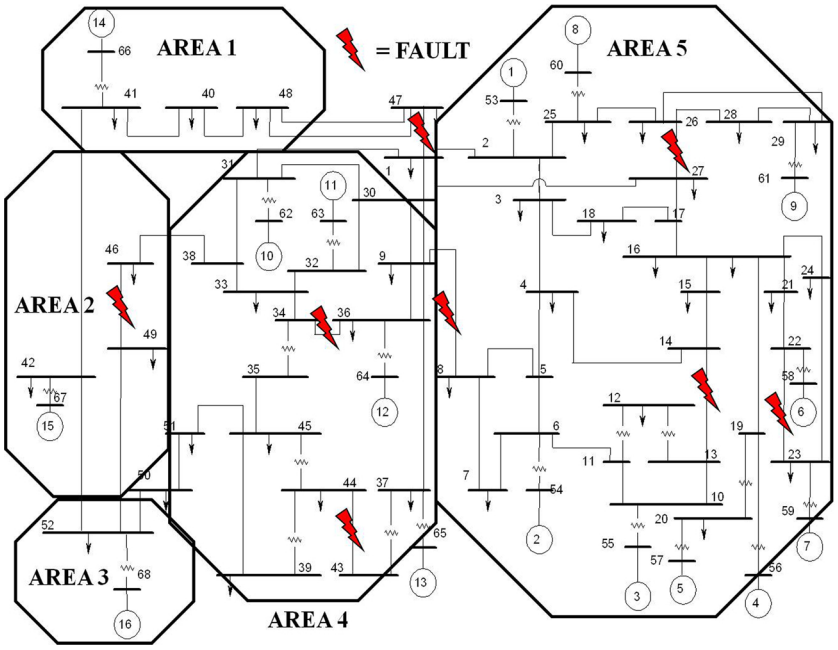

Fig. 7. Single line diagram to the IEEE 16-generator 68-bus system.

Table 1
Inter-area modes

Mode	Eigenvalue base case	Eigenvalue with PSS
1	$-0.0546 \pm 2.5093\,i$	$-1.3341 \pm 2.44\,i$
2	$-0.0468 \pm 3.0628\,i$	$-0.4538 \pm 3.16\,i$
3	$-0.1542 \pm 3.9711\,i$	$-0.6356 \pm 4.49\,i$
4	$-0.2391 \pm 4.9545\,i$	$-0.5499 \pm 5.36\,i$

Table 2
Locations of faults

Fault	from bus	to bus	Fault	from bus	to bus
1	1	47	5	26	27
2	8	9	6	34	36
3	13	14	7	43	44
4	22	23	8	46	49

shown in Fig. 6, where the fitting to the spectral coefficients and loci of the roots are given by restriction eig $(\mathrm{Re}\{\boldsymbol{G}(s,\tau_c)|_{s\to a_c} \circ \Delta\boldsymbol{G}(s,\tau)|^{\perp}_{s\to\Delta a}\}) > \{0\}$ to $a_c = -\sigma_c + i\omega_c$ with $\sigma_c > 0$ [34]. From these results, we identify a set of parameters to (32), which guarantees the modal stability conditions in intervals $\{[\tau_{\min}, \tau_{\max}]\} = \{[0, 0.82]\}$ and $\{[q_{\min}, q_{\max}]\} = \{[0, 2.42]\}$. Thus, the subscripts min and max denote, respectively, the lower and upper bounds of the generated stability margins. In consideration, this illustrative test helps to assess the proposed approach into perturbed systems applications with the equivalent representation of linear state-space models, where multivariable datasets from multiple system responses and stability conditions are treated. The EOFs analysis and vector fitting procedure are algorithms of low computational burden. This fact allows the proposed algorithm to be used in wide-area systems applications for processing large databases. New studies and tests applying the proposed approach to nonlinear systems responses will be considered as future work.

4.2. IEEE 16-generator 68-bus test system

Results of new studies on perturbed time-delays and sensitivity analysis using multivariable signals and its inter-area dissipativity at interconnected power networks are here presented. The IEEE 16-generator 68-bus system shown in Fig. 7, with network characteristics given in [37] is used as test network. The system consists of five areas interconnected between them, as it is also illustrated. Table 1 synthesizes the eigenvalues for the base case condition. To the proposed analysis, the system modeling is structured considering that each generator is represented by a subtransient model. The load models are defined as constant impedances and the interconnected transmission network is reduced to generator internal nodes. Several three-phase fault scenarios on tie-lines are simulated as transient conditions altering its operating equilibrium to study the system vulnerability and modal resilience by distributed perturbations. In Table 2, are given the buses and the number of faults that have been arbitrarily involved, which are highlighted in Fig. 7. The voltage magnitudes recorded in all system's buses as discrete data series, using a sampling interval of $\Delta t = 0.01$ s over a $t = 100$ s window, have been analyzed as demonstrative

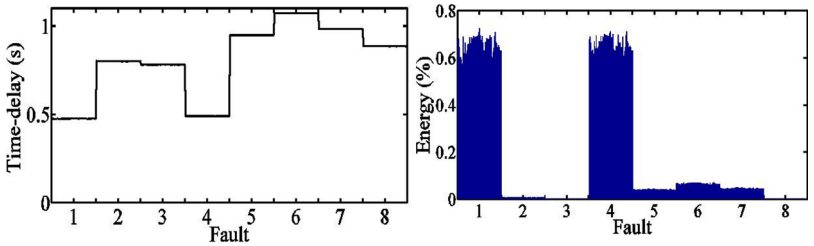

Fig. 8. Variations associated with the dominant oscillation mode. Left: perturbed time-delays. Right: energy distribution.

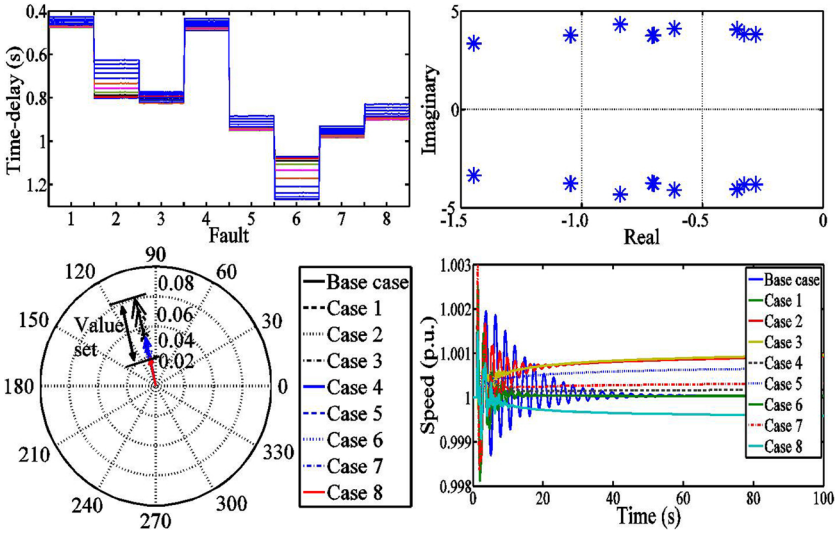

Fig. 9. Left-upper: Intervals of time-delays. Right-upper: Loci of the roots. Left-lower: phase shifting distribution (mode shape). Right-lower: rotor speed deviation in generator 1.

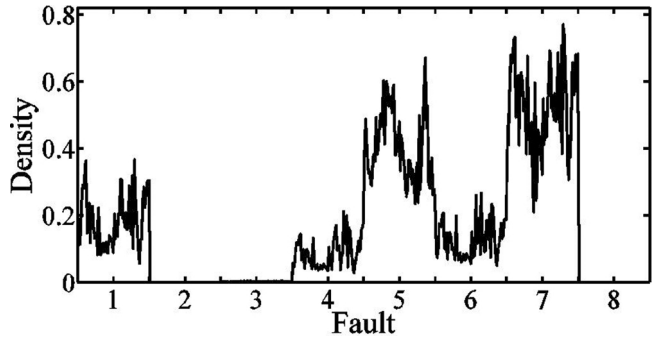

Fig. 10. Joint-probability density function to the modal instability condition.

provision. Additionally, the machine speed deviations have also been considered. For illustration, the multiple faults are applied at time $t = 1.1$ s and clearing in time $t = 1.15$ s by opening their tie-lines. It is assumed that there is space-time overlap between measurements and sensors locations to define the spectral overlap among multiple system responses. In order to examine the potential usefulness of the algorithm proposed in Section 3.5, Fig. 8 shows the estimated distribution of perturbed time-delays and energy contributions. These results have been determined for each transient condition regarding to identified dominant inter-area oscillation mode. Note that during random inter-area transient conditions, there exists several intervals of time-delays and energy contributions. The multivariable time-delay margins to infer the stable system condition associate to delayed communication channels, the processing of large datasets, waveforms propagation, and other factors are possible from the proposed methodology since we are considering a time-delay interval based on the spatial geometry of multiple system responses. Thus, distributed margins of controlled dynamic security by multivariable modal instability regarding to energy contributions and intervals of phase shifting from inter-area perturbations can be inferred. Therefore, the lower and upper bounds of security margins are given in intervals $\{[\tau_{min}, \tau_{max}]\} = \{[0, 1.25]\}$ seconds, and $\{[\text{Energy}_{min}, \text{Energy}_{max}]\} = \{[0, 32.5]\}$ in percentage of the total energy liberated by the transient processes. Hence, the distributed uncertainty of time-delay perturbed power systems have been used to determine stable system conditions. In addition to this, it is noted that by multiple linear combinations among these intervals, and maintaining the average balance of energy contributions and resulting geometric distribution of spatial phase shifting, the modal dynamic security might be preserved. Then, to illustrate this, in Fig. 9 and Table 1, are shown several test results under stable system condition considering the balance of modal energy contribution due to multiple distributed variations in damping factor rations. However, the resulting geometry of phase shifting from a controllable geometric phase shifting filter can also be implemented as future research. This condition is validated from the structured mode shape, machine speed deviation and movements to the loci of roots also included in Fig. 9. These findings were generated employed the multiple transient responses via emulation of PSS devices that usually work with speed variation of the generators as proposed in [14]. For simplicity and assuming proper conditions of the methodology developed in this paper, the implementation of PSS devices have been arbitrarily considered in buses $\{13 - 16\}$, without employing optimal search algorithms. Note that Fig. 9 shows the multivariable local distribution and variation of the perturbed time-delays, where our result indicates that faults $\{2, 6\}$ have major time-delay and that these are associated to tie-lines between areas 4 and 5, respectively. Likewise, the probabilistic analysis of the modal instability condition and modal resilience is shown in Fig. 10, where the joint-probability density function estimated by form (31) is presented. From the statistical representations given in Fig. 10, it can be noticed that the modal instability and stability condition are inferred by the causal variability regarding to multiple perturbations in several locations. Thus, both conditions are associated to the distributed causality derived by faults $\{5, 7\}$, and faults $\{2, c, 8\}$ respectively. Therefore, these variations are used to define margins of proximity and vulnerability to modal instability as causal relationships prediction. From it, we note that faults $\{5, 7\}$ are associated to areas 4 and 5, which presents the most significant effects in proximity to inter-area modal instability condition by distributed uncertainty. The results given in Fig. 10 quantitatively measure modal resilience in power systems, which can be used for network restoration planning or wide-area damping control design from energy control centers through experticies of past events. Specifically, the density function illustrates the impact of the modal oscillation using the distributed resilience for interconnected power systems. The main drawbacks of the proposed method during its practical application are associated to treat the modal observability, in which case should be considered in detail and as special attention the types and numbers of faults to use, including their spatial locations and directions. Additionally, the identification of inter-area coherence between generators from an empirical perspective will be also considered. These enhancements will be developed in future research.

5. Conclusion

This paper has presented a statistical inference algorithm to empirically evaluate and analyze the operational stability condition of time-delay perturbed power systems. The proposed approach employs the empirical modeling of time-delay dynamic systems through rational function fitting treating the distributed uncertainty and perturbed time-delays by multivariable polynomial intersection and function composition via datasets. This approach overcomes the drawbacks of computational burden, linear independence, and inter-area geometry of time-delays in conventional methods to analyze multiple-input, multiple-output dynamic systems. The proposed algorithm, which combines both statistical aspects and vulnerability studies, contributes to infer controlled security conditions and the distributed dynamic causality of coordinated inter-area intermissions for interconnected power systems. From the simulation results, it is shown that the proposed method can be efficiently used to analyze large datasets collected from multiple sources. A practical analysis of multi-scale signal sensitivity by spectral energy overlap at frequency-domain empirical orthogonal functions to assess the modal resilience and quantify distributed uncertainties of interconnected power systems is also presented. It is worth mentioning that this approach helps to define detailed studies on the inter-area geometry of perturbed time-delays in wide-area monitoring schemes.

Author contributions

P. Esquivel: Conceptualization, Methodology. G. Romero: Investigation. F. Ornelas-Tellez: Visualization. E. N. Reyes: Investigation. Carlos E. Castañeda: Reviewing and Editing O. A. Morfin: Supervision and Validation.

References

[1] Y. Susuki, I. Mezic, Nonlinear Koopman modes and power system stability assessment without models, IEEE Trans. Sustain Energy 29 (2) (2014) 899–907.

[2] S.N. Sarmadi, V. Venkatasubramanian, Electromechanical mode estimation using recursive adaptive stochastic subspace identification, IEEE Trans. Power Syst. 29 (1) (2014) 349–358.

[3] S. Zhao, K. Loparo, Forward and backward extended prony (FBEP) method for power systems small-signal stability analysis, IEEE Trans. Power Syst. 32 (5) (2017) 3618–3626.

[4] E. Barocio, B. Pal, N. Thornhill, A. Messina, A dynamic mode decomposition framework for global power system oscillation analysis, IEEE Trans. Power Syst. 30 (6) (2015) 2902–2912.

[5] I. Cabrera, E. Barocio, R. Betancourt, A. Messina, A semi-distributed energy-based framework for the analysis and visualization of power system disturbances, Electric Power Syst. Res. 143 (1) (2017) 339–346.

[6] Z. Wang, C. Shen, F. Liu, Probabilistic analysis of small signal stability for power systems with high penetration of wind generation, IEEE Trans. Sustain. Energy 1 (1) (2016) 1–12.

[7] L. Cai, X. Tian, S. Chen, Monitoring nonlinear and non-Gaussian processes using Gaussian mixture model-based weighted kernel independent component analysis, IEEE Trans. Neural Learn. Syst. 28 (1) (2017) 122–135.

[8] R. Singh, B. Pal, R. Jabr, Statistical representation of distribution system loads using Gaussian mixture model, IEEE Trans. Power Syst. 25 (1) (2010) 29–37.

[9] X. Xu, X. He, Q. Ai, R. Qiu, A correlation analysis method for power systems based on random matrix theory, IEEE Trans. Smart Grid 8 (4) (2015) 1811–1820.

[10] V. Peric, X. Bombois, L. Vanfretti, Optimal signal selection for power system ambient mode estimation using a prediction error criterion, IEEE Trans. Power Syst. 31 (4) (2016) 2621–2633.

[11] L. Cai, N. Thornhill, S. Kuenzel, B. Pal, Wide-area monitoring of power systems using principal component analysis and k-nearest neighbor analysis, IEEE Trans. Power Syst. PP 99 (2018) 1–10.

[12] P. Esquivel, C. Castaneda, Spatio-temporal statistical identification methodology applied to wide-area monitoring schemes in power systems, Electric Power Syst. Res. 111 (1) (2014) 52–61.

[13] B.P. Padhy, Adaptive latency compensator considering packet drop and packet disorder for wide area damping control design, Electrical Power Energy Syst. 106 (1) (2019) 477–487.

[14] T. Prakash, V. Singh, S. Mohanty, A synchrophasor measurement based wide-area power system stabilizer design for inter-area oscillation damping considering variable time-delays, Electrical Power Energy Syst. 105 (1) (2019) 131–141.

[15] M.E. Bento, A hybrid procedure to design a wide-area damping controller robust to permanent failure of the communication channels and power system operation uncertainties, Electrical Power Energy Syst. 110 (1) (2019) 118–135.

[16] L. Cheng, G. Chen, W. Gao, F. Zhang, G. Li, Adaptive time delay compensator (ATDC) design for wide-area power system stabilizer, IEEE Trans. Smart Grid 5 (6) (2014) 2957–2966.

[17] G. Tzounas, M. Liu, M. Murad, F. Milano, Stability analysis of wide area damping controllers with multiple time delays, Advanced Modelling for Power System Analysis and Simulation (AMPSAS) - SFI Investigator Program (2016-2021), Dublin, Ireland, 2018, pp. 01–06.

[18] X. Zhang, C. Lu, X. Xie, Z. Dong, Stability analysis and controller design of a wide-area time-delay system based on the expectation model method, IEEE Trans. Smart Grid 7 (1) (2016) 520–529.

[19] W. Yao, Q. Hu, J. Wen, S. Cheng, Delay-dependent stability analysis of the power system with a wide-area damping controller embedded, IEEE Trans. Power Syst. 26 (1) (2011) 233–240.

[20] A. Molina-Cabrera, M. Rios, Y. Besanger, N. HadjSaid, A latencies tolerant model predictive control approach to damp inter-area oscillations in delayed power systems, Int. J. Electrical Power Energy Syst. 98 (1) (2018) 199–208.

[21] Y. Shiozaki, M. Liu, M. Murad, F. Milano, Design of a wide-area damping controller considering communication time delays, 2018 Power Systems Computation Conference (PSCC), Dublin, Ireland, 2017, pp. 01–07.

[22] M. Fu, A. Olbrot, M. Polis, Robust stability for time-delay systems: the edge theorem and graphical test, IEEE Trans. Automatic Control 34 (8) (1989) 813–820.

[23] G. Romero, J. Collado, Robust stability of interval plants with perturbed time delay, Proc. of the American Control Conference, Seattle, Washington USA, 1995, pp. 326–327.

[24] G. Romero, Robust stability analysis for a class of linear time-delay systems, Proc. of the European Control Conference, Kos, Greece, 2007, pp. 5610–5615.

[25] A. Metel'skii, Spectral reducibility of delay differential systems by a dynamic controller, Control Theory Differential Equations 47 (11) (2011) 1642–1659.

[26] J. Wallance, R. Dickinson, Empirical orthogonal representation of time series in the frequency domain. Part I: theoretical considerations, J. Appl. Meteorol. 11 (6) (1972) 887–892.

[27] T. Kin, Frequency-domain Karumen-Loeve method and its application to linear dynamic systems, Am. Inst. Aeronaut. Astronaut. J. 36 (11) (1998) 2117–2123.

[28] P. Esquivel, C. Castaneda, Reduced-order equivalent model to large power networks derived from its spectral dispersion, Electric Power Syst. Res. 143 (1) (2017) 244–251.

[29] P. Moreno, A. Ramirez, Implementation of the numerical Laplace transform: a review, IEEE Trans. Power Del. 33 (4) (2008) 2599–2609.

[30] R. Schumacher, G. Oliveira, An optimal vector fitting method for estimating frequency-dependent networks equivalents in power systems, Electric Power Syst. Res. 150 (1) (2017) 96–104.

[31] J. Qi, K. Sun, W. Kang, Optimal PMU placement for power system dynamic state estimation by using empirical observability Gramian, IEEE Trans. Power Syst. 30 (4) (2015) 2041–2054.

[32] T. Kailath, Linear Systems, 156, Prentice-Hall Englewood Cliffs, NJ, 1980.

[33] A. Thakallapelli, S. Kamalasadan, Alternating direction method of multipliers (admms) based distributed approach for wide-area control, IEEE Trans. Ind. Appl. 55 (3) (2019) 3215–3227.

[34] Y. Hu, W. Wu, A. Gole, B. Zhang, A guaranteed and efficient method to enforce passivity of frequency dependent network equivalents, IEEE Trans. Power Syst. 1 (1) (2016) 01–08.

[35] P. Vahdati, A. Kazemi, M. Amini, L. Vanfretti, Hopf bifurcation control of power system nonlinear dynamics via a dynamic state feedback controller-part i: theory and modeling, IEEE Trans. Power Syst. 32 (4) (2017) 3217–3228.

[36] N. Rodgers, Learning to Reason: An Introduction to Logic, Sets, and Relations, John Wiley-Sons, Inc, Hanover College, NJ, USA, 2000.

[37] G. Rogers, Power System Oscillations, Springer US, Springer Science and Business Media New York, USA, 2000.